Journal Pre-proofs

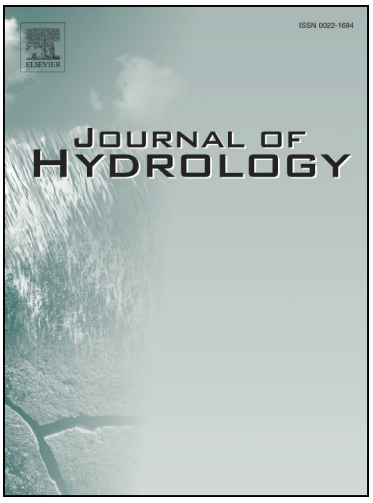

Research papers

Alternative methods to determine the δ ^{2}H-δ ^{18}O relationship: an application to different water types

C. Marchina, G. Zuecco, G. Chiogna, G. Bianchini, L. Carturan, F. Comiti, M. Engel, C. Natali, M. Borga, D. Penna

PII: S0022-1694(20)30411-X
DOI: https://doi.org/10.1016/j.jhydrol.2020.124951
Reference: HYDROL 124951

To appear in: *Journal of Hydrology*

Received Date: 24 December 2019
Revised Date: 9 April 2020
Accepted Date: 10 April 2020

Please cite this article as: Marchina, C., Zuecco, G., Chiogna, G., Bianchini, G., Carturan, L., Comiti, F., Engel, M., Natali, C., Borga, M., Penna, D., Alternative methods to determine the δ ^{2}H-δ ^{18}O relationship: an application to different water types, *Journal of Hydrology* (2020), doi: https://doi.org/10.1016/j.jhydrol.2020.124951

Alternative methods to determine the δ^2H-$\delta^{18}O$ relationship: an application to different water types

Marchina C.[1,2], Zuecco G.[2], Chiogna G.[3,4], Bianchini G.[1], Carturan L.[2,5], Comiti F.[6], Engel M.[6], Natali C.[7], Borga M.[2], Penna D.[8]

[1]Department of Physics and Earth Science, University of Ferrara, Italy

[2]Department of Land, Environment, Agriculture and Forestry, University of Padova, Italy

[3]Chair of Hydrology and River Basin Management, Technical University of Munich, Germany

[4]Department of Geography, University of Innsbruck, Austria

[5]Department of Geosciences, University of Padova, Italy

[6]Faculty of Science and Technology, Free University of Bozen-Bolzano, Italy

[7]Department of Earth Sciences, University of Florence, Italy

[8]Department of Agriculture, Food, Environment and Forestry, University of Florence, Italy

Correspondence to: Giulia Zuecco (giulia.zuecco@unipd.it), Department of Land, Environment, Agriculture and Forestry, University of Padova, via dell'Università 16, 35020 Legnaro (PD), Italy

First submitted for publication in Journal of Hydrology: 24 December, 2019

Resubmitted: 9 April, 2020

Highlights

- Uncertainty in slopes of mixed waters is not explained by the experimental error
- Stream and spring isotopic data have significant differences in the slopes
- Evaporated soil water does not significantly affect the δ^2H-$\delta^{18}O$ relationship

Abstract

The Ordinary Least Squares (OLS) regression is the most common method for fitting the δ^2H-$\delta^{18}O$ relationship. Recently, various studies compared the OLS regression with the Reduced Major Axis (RMA) and Major Axis (MA) regression for precipitation data. However, no studies have investigated so far the differences among the OLS, RMA and MA regressions for water types prone to evaporation, mixing, and redistribution processes. In this work, we quantified the differences in terms of slopes and intercepts computed by the OLS, RMA, and MA methods for rainfall, snow and ice, stream, spring, groundwater, and soil water, and investigated whether the magnitude of such differences is significant and dependent on the water type, the datasets statistics, geographical or climatic characteristics of the study catchments.

Our results show that the differences between the regression methods were largest for the isotopic data of some springs and some stream waters. Conversely, for rainfall, snow, ice, and melt waters datasets, all the differences were small and, particularly, smaller than their standard deviation. Slopes and intercepts computed using the different regression methods were statistically different for stream water (up to 70.4%, n=54), followed by groundwater, springs, and soil water. The results of this study indicate that a thorough analysis of the δ^2H-$\delta^{18}O$ relationship in isotope hydrology studies is recommended, as well as considering the measurement errors for both δ^2H and $\delta^{18}O$, and the presence of outliers. In case of small measurement errors and no significant differences between the slopes, we suggest the application of the widely used OLS regression. Conversely, if the computed slopes are significantly different, we recommend investigating the possible reasons for such discrepancies and prefer the RMA over the MA approach, as the latter tends to be more sensitive to data with high leverage (i.e., data points with extreme $\delta^{18}O$ values).

Keywords: stable water isotopes; Ordinary Least Squares regression; Major Axis regression; stream water; Global Meteoric Water Line; catchment.

1. Introduction

The relationship between δ^2H and $\delta^{18}O$ values (the isotopic ratios, R, for $^2H/^1H$ and $^{18}O/^{16}O$ are expressed as δ notation, where $\delta = (\frac{R_{sample}}{R_{standard}} - 1) \times 1000$) of water samples is commonly defined by a simple linear regression. In hydrological studies, the Ordinary Least Squares (OLS) method is the most common statistical regression for fitting the δ^2H-$\delta^{18}O$ relationship (Dansgaard, 1964; Hughes and Crawford, 2012; Carr 2012; Crawford et al., 2014; Boschetti et al., 2019; Putman et al., 2019). Conventionally, around 60 years ago Craig (1961) determined for the first time the δ^2H-$\delta^{18}O$ relationship of meteoric water at the global scale, the so called Global Meteoric Water Line (GMWL). Local meteoric water lines (LMWL) can then be computed at the regional scale. LMWLs are used to characterise the vapour masses originating precipitation over a certain area (e.g., Peng et al., 2015; Xu et al, 2019; Zannoni et al., 2019), determine the origin of groundwater and its interaction with surface waters (e.g., Rozanski et al., 1993; Wassenaar et al., 2011; Tan et al., 2016), and evaluate hydroclimatic processes in isotope-enabled climate models (e.g., Putman et al., 2019).

In many scientific fields, the OLS regression is not considered a proper method to define a linear relationship because there are no measurement errors associated with the independent variable (Cantrell, 2008; Smith, 2009; Carr, 2012; Harper, 2014; Keles, 2018). Conversely, alternative regression methods, such as the Reduced Major Axis (RMA, also known as the line of organic correlation and the geometric mean regression) and the Major Axis (MA, also known as least normal squares and orthogonal regression), consider the presence of errors for the independent variable. In the RMA regression the area of the triangle formed by the line and the data point is minimised, whereas in the MA, the orthogonal (perpendicular) distance from the line to the data point is minimised (Fig. 1). The RMA regression is symmetric, i.e., a single line defines the bivariate relationship regardless of which variable is "x" and which is "y", while the OLS regression is asymmetric, so that the slope and the resulting interpretation change when the variables assigned to "x" and "y" are reversed (Rollinson, 1993; Helsel and Hirsch, 2002; Smith, 2009; Carr, 2012).

Basically, the important difference between the OLS regression method and the RMA and MA regression methods is that the former minimizes the error only for the ”y” variable whereas the two latter minimize the errors both in the ”x” and in the ”y” direction (Helsel and Hirsch, 2002). This makes, in principle, RMA and MA approaches more suitable to interpolate isotopic data as the two isotopes are independent from each other.

RMA and MA have also been proposed by IAEA (1992) for water isotopic data, and recently these approaches have been applied to LMWLs (e.g., Sánchez-Murillo et al., 2015; Kaseke et al., 2016; Hervé-Fernández et al., 2016; Vreča and Malenšek, 2016; Le Duy et al., 2018; Hollins et al., 2018; Qu et al., 2018; Wang et al., 2019). Various studies in isotope hydrology proposed the RMA and MA regressions as statistical methods that could be applied when a relationship is being sought between two variables, which are related by underlying physical processes (Argiriou and Lykoudis, 2006; Hughes and Crawford, 2012; Crawford et al., 2014; 2017). Argiriou and Lykoudis (2006) were among the ones to propose the RMA regression as an alternative method to define the LMWL in Greece. Hughes and Crawford (2012) and Crawford et al. (2014) tested for the first time the hypothesis that the three different regression methods (the OLS, RMA, and MA) applied to the $\delta^{2}H$-$\delta^{18}O$ relationship of precipitation give quite different slopes and intercepts. Crawford et al. (2014) concluded that the RMA and MA regressions produced larger slopes than the OLS method, with the largest differences being for precipitation datasets from oceanic islands, coastal and Mediterranean sites, whereas differences in slope and intercepts between the various methods were smaller for continental sites. In addition, the RMA regression produced slopes in between those determined by the OLS and MA regressions, with the smallest values of root mean squared errors, indicating that the RMA method is more suitable for the computation of LMWLs compared to the MA regression (Crawford et al., 2014).

Obtaining reliable parameters for LMWLs as well as regression lines for isotopic data of other water types is particularly important for research studies focusing on groundwater recharge (e.g., Gonzalez-Trinidad et al., 2017; Oiro et al., 2018), evaluating the effect of evaporation processes on

surface waters (e.g., Florea et al., 2017; Sharma et al., 2017; Shi et al., 2019) or investigating source waters based on evaporation lines (e.g., Evaristo et al., 2015; Javaux et al., 2016; Benettin et al., 2018). For example, the visual inspection of the overlap between groundwater isotopic data and LMWL allows to better understand groundwater recharge processes (Boschetti et al., 2019). Furthermore, evaporation processes are usually evaluated in terms of deviation of samples from the GMWL or the relative LMWLs (Sharma et al., 2017; Shi et al., 2019). Penna et al. (2014; 2017b) compared the slopes and intercepts (based on the OLS regression) of isotopic data for different water types (snowmelt, ice melt, winter snowpack, stream water and groundwater) to the LMWL and assessed climatic conditions and/or evaporation effects in a glacierized catchment and in a snowmelt-dominated catchment of the Italian Alps. Similarly, but in a different environment, Klaus et al. (2015) used the slope and intercepts of OLS regression lines to highlight the role of the riparian zone to control baseflow in low-relief, forested catchments.

Recently, Boschetti et al. (2019) defined a new LMWL for northern Chile, computed by another method, called the error-in-variables (EIV) approach. They compared the LMWL obtained by the EIV method with the ones computed by the OLS, RMA, and MA regressions (and their weighted versions). They concluded that the EIV regression, which considers the combined standard deviation of the $\delta^{18}O$ and $\delta^{2}H$ values, produced a LMWL with a slope similar to those obtained with the other approaches. However, the EIV approach was considered more suitable than the OLS regression, because the EIV method accounts for measurements errors in both $\delta^{2}H$ and $\delta^{18}O$ (Boschetti et al., 2019).

Beyond the studies mentioned above, we are not aware of any research that applied OLS, RMA, and MA regression methods to isotopic data from different water types prone to evaporation, mixing and redistribution processes, analysing the factors potentially affecting the differences between the three methods. Therefore, in this work, we aim to:

1) quantify the differences in slopes and intercepts in the δ^2H-$\delta^{18}O$ relationship computed by the OLS, RMA, and MA methods for various water types (i.e., snow, ice and melt waters, stream water, shallow groundwater, spring, and soil waters);

2) investigate whether the differences in slopes and intercepts computed through the three regression methods are significant and affected by water type, datasets statistics, geographical or climatic characteristics of the selected catchments;

3) provide recommendations about the regression method to be applied in isotope hydrology studies.

2. Materials and methods

2.1. Selected study sites in Italy and sampling of water sources

In this study, the OLS, RMA, and MA regressions were applied to isotopic data collected from different water sources in nine catchments in north-eastern Italy (Fig. 2; Table 1). We chose these study sites for their different drainage areas as well as climatic and hydrological characteristics. The main features of the catchments, along with details of the sampled water sources are presented in Table 1. The study areas can be divided into: i) large basins (Po River, and Adige River); ii) mesoscale and nested catchments (Posina River at two outlets and its Ressi Creek sub-catchment, Vermigliana River, and Saldur/Saldura River); iii) small catchments (Noce Bianco Creek, and Rio Vauz Creek).

In some catchments (i.e., Posina, Rio Vauz, Noce Bianco, Saldur, and Vermigliana) the isotopic composition was measured for different water sources at multiple sampling sites during various hydrological conditions (dry, wet, melt, and non-melt periods). Selected data include the isotopic composition of rain water, snow, glacier ice, melt water (snowmelt and glacier melt were grouped together), surface (stream) water, spring water, groundwater, and soil water, collected between 2010 and 2017 (Table 1; Fig. 3). Stream waters were sampled in all the nine catchments. Stream waters were sampled both manually and by automatic water samplers depending on the accessibility of the

sampling sites. Snapshot manual sampling campaigns were carried out in the Po River from 2012 to 2017 (Marchina et al., 2015; Marchina et al., 2016; Marchina et al., 2017; Marchina et al., 2019) and in the Adige River in 2013-2017 (Natali et al., 2016; Chiogna et al., 2018). In this study, in order to compare the Po and Adige stream water data to data from the other catchments, we selected only samples collected multiple times in the Po River at Pontelagoscuro and in the Adige River at Andriano, Verona, and Boara Pisani (Table 1). Stream water samples were collected monthly in Posina, Ressi, and Vermigliana at various sampling sites (Chiogna et al., 2014; Penna et al., 2015), whereas generally stream water samples were retrieved monthly from May to October in the snow- or glacier-melt dominated high-elevation catchments (Rio Vauz, Saldur and Noce Bianco). Additional stream water samples were collected at sub-daily temporal resolution during rainfall events in Vermigliana (Cano-Paoli et al., 2019), Posina, Ressi (Penna et al., 2015) and Bridge Creek catchment (BCC), a Rio Vauz subcatchment (Penna et al., 2017b), and snow- or glacier-melt-induced runoff events in Saldur (Engel et al., 2016), BCC (Penna et al., 2016) and Noce Bianco (Zuecco et al., 2019a). Bulk rain water samples were collected approximately monthly in Ressi, and monthly from May to October in high-elevation catchments (Rio Vauz, Saldur and Noce Bianco). Rain water was sampled by 5-l high-density polyethylene bottles, equipped with a funnel and a layer of mineral oil to prevent evaporation. Samples bottles were capped and moved to the laboratories, where bulk samples were transferred into 50-ml high-density polyethylene bottles. Spring water samples were manually collected monthly from May to October, in Saldur (four sites), Rio Vauz (two sites) and Noce Bianco (one site), or during a snapshot campaign in summer 2012 at 46 springs in a 36-km^2 catchment comprising Noce Bianco (Carturan et al., 2016). Shallow groundwater was sampled in six piezometers monthly in Ressi (Penna et al., 2015), five piezometers monthly from May to October in BCC (Penna et al., 2016; Zuecco et al., 2019b), and monthly in one well in Vermigliana (Chiogna et al., 2014). Soil water was extracted by suction cups from two sites (one in the hillslope, and one in the riparian zone, sampled occasionally during wet conditions in summer) in BCC, and by suction cups (three sites, one in the riparian zone and two in the hillslope, sampled

monthly) and cryogenic vacuum distillation (two sites, one in the riparian zone and one in the hillslope, sampled monthly from May to October) at different depths (10, 30, 40 and 60 cm) in Ressi.

All the water samples for isotopic analyses were collected in 50-100 ml high-density polyethylene bottles, sealed without head space, whereas soil samples for the cryogenic extraction were collected in 12-ml glass vials. Cryogenic vacuum distillation was performed at the Faculty of Science and Technology of the Free University of Bozen-Bolzano, using the cryogenic method developed by Koeniger et al. (2011). All the samples were stored at 4 °C until the isotopic analyses.

2.2. Isotopic analyses

The isotopic composition was determined for most of the samples by laser spectroscopes, following the procedures reported in Penna et al. (2010; 2012). All the samples were calibrated with standards relative to the Vienna Standard Mean Ocean Water. Samples from Rio Vauz, Posina, Noce Bianco, and Saldur were analysed by the liquid water isotope analyser (off-axis integrated cavity output spectroscopy method, model DLT-100, manufactured by Los Gatos Research, California, USA) at the Forest Hydrology Laboratory of the Dept. of Land, Environment, Agriculture and Forestry of the University of Padova. The average standard deviation of 2094 samples was 0.5‰ for δ^2H and 0.08‰ for $\delta^{18}O$ (Penna et al., 2016). Soil water samples collected in Ressi and extracted by cryogenic vacuum distillation were analysed by the water isotope analyser (cavity ring-down spectroscopy method, model L2130-i, manufactured by Picarro Inc., California, USA) at the Faculty of Science and Technology of the Free University of Bozen-Bolzano. Analytical uncertainty of δ^2H and $\delta^{18}O$ measurements was lower than 1.0‰ and 0.20‰, respectively. Samples collected from Po and Adige rivers were analysed by the liquid water isotope analyser (cavity ring-down spectroscopy method, model 24-d, manufactured by Los Gatos Research, California, USA) at the Dept. of Physics and Earth Science of the University of Ferrara. The average standard deviation of 366 samples was 0.7‰ for δ^2H and 0.14‰ for $\delta^{18}O$. Samples

collected in Vermigliana were analysed by two isotope ratio mass spectrometers depending on their availability (SIRA II, VG Isogas, Middlewich, UK, and Isoprime, Manchester, UK). Analytical uncertainty (one standard deviation of reproducibility) of δ^2H and $\delta^{18}O$ measurements was 2.0‰ and 0.20‰, respectively (Chiogna et al., 2014).

2.3. Selection of European river data from the GNIR database

In order to detect the possible effects of climatic and geographical characteristics on the regression parameters, the OLS, RMA, and MA regressions were also applied to the European river data available from the global database of riverine stable water isotopes (Global Network of Isotopes in Rivers; Halder et al., 2015). The GNIR database is an electronic repository of river water isotopic data associated with geographical, physical, and chemical parameters. The GNIR database is publicly accessible online through the web-based Water Isotope System for Data Analysis, Visualization and Electronic Retrieval (WISER) interface at https://nucleus.iaea.org/wiser. We selected only stream water data comprising both δ^2H and $\delta^{18}O$ and the main characteristics of the catchment (such as latitude, longitude, and elevation of the sampling sites). In addition, information not included in the GNIR database (i.e., mean annual precipitation, mean annual temperature, and catchment size) was retrieved from literature for the selected catchments (e.g., Pawellek et al., 2002; Rank et al., 2006; Miljević et al., 2008; Halder et al., 2013). In total, we retrieved isotopic data from 34 European river sites (Table S1).

2.4. The OLS, RMA, and MA regressions

We applied the OLS, RMA, and MA regressions to each water type in each catchment (study catchments and selected data from the GNIR database). To fit the OLS, RMA, and MA regressions to δ^2H and $\delta^{18}O$ data (expressed in ‰), we used the equations reported in Helsel and Hirsch (2002) and Crawford et al. (2014). In the equations reported below, x and y represent $\delta^{18}O$ and δ^2H, respectively, n is the sample size, and r is the Pearson correlation coefficient.

In the OLS regression, the sum of the squares of the vertical distances from the best fitted line to the sampling points is minimized (Fig. 1). Based on this minimization, $slope_{OLS}$ depends on *r*, and the ratio between the standard deviation (*sd*) determined for the *y* and *x* variables, as follows:

$$slope_{OLS} = r \times \frac{sd_y}{sd_x} \quad (1)$$

The RMA regression is based on the minimization of the sum of the areas of the right triangles built with the sampling points and the best fit straight line (Fig. 1). $slope_{RMA}$ was determined as:

$$slope_{RMA} = sign[r]\frac{sd_y}{sd_x} \quad (2)$$

where $sign[r]$ represents the algebraic sign of the Pearson correlation coefficient, *r*.

Based on Equations 1 and 2, the relationship between $slope_{OLS}$ and $slope_{RMA}$ can be written as:

$$slope_{OLS} = r \times slope_{RMA} \quad (3)$$

This relationship between $slope_{OLS}$ and $slope_{RMA}$ implies that for positive correlations, such as between δ^2H and $\delta^{18}O$, $slope_{RMA}$ will always be larger than $slope_{OLS}$.

In the MA regression, the sum of the squared perpendicular distances from each sampling point to the best fitted line is minimized (Fig. 1). Thus, $slope_{MA}$ was obtained as:

$$slope_{MA} = -A + \frac{\sqrt{r^2 + A^2}}{r} \quad (4)$$

where $A = 0.5(\frac{sd_x}{sd_y} - \frac{sd_y}{sd_x})$.

The intercept was computed using the same equation for the three regression methods:

$$intercept = \frac{\sum_{i=1}^{n} y_i}{n} - slope\frac{\sum_{i=1}^{n} x_i}{n} \quad (5)$$

The standard errors (SE) of the slope and the intercept were calculated following the equations by Volk (1958):

$$SE_{slope} = \frac{\sqrt{\frac{\sum_{i=1}^{n}(y_i - \hat{y}_i)^2}{n-2}}}{\sqrt{\sum_{i=1}^{n}(x_i - \hat{x}_i)^2}} \quad (6)$$

$$SE_{intercept} = SE_{slope}\sqrt{\frac{\sum_{i=1}^{n} x_i^2}{n}} \quad (7)$$

where $\hat{y}_i$ represent predicted $\delta^{18}O$ data ($\hat{y}_i = slope \times x_i + intercept$).

Following Isobe et al. (1990) and Feigelson and Babu (1992), we also calculated the standard deviations of the slope and intercept obtained using the three different regression methods. This approach is suggested when the nature of the scatter about a linear relationship is unknown, i.e., as specified by Isobe et al. (1990) "the intrinsic scatter of the data dominates any errors arising from the measurement process".

Error propagation from the observations which are affected by measurement errors ($\Delta\delta^2H$ and $\Delta\delta^{18}O$) was also applied to estimate the uncertainty in the slope and intercept. The uncertainty on the quantity of interest (Q) was calculated using the following equation (Fornasini, 2008):

$$\Delta Q = \sqrt{\sum_{i=1}^{n} \frac{\partial Q}{\partial X_i} \Delta X_i} \quad (7)$$

where ΔQ is the error in the quantity of interest (in our case slope or intercept), and X_i is the analytical uncertainty in the measurement of δ^2H and $\delta^{18}O$. For this analysis, we focused only on the case of the OLS regression by applying the error propagation to the various datasets, using the specific analytical uncertainty of each isotopic analyser. In order to be more conservative in our data analyses, we considered an analytical uncertainty of 1.0‰ (δ^2H) and 0.20‰ ($\delta^{18}O$) for the isotopic data obtained with the laser spectroscopes at the University of Padova, University of Ferrara and Free University of Bozen-Bolzano (Penna et al., 2016). For the Vermigliana data, we used the analytical uncertainty of 2.0‰ (δ^2H) and 0.20‰ ($\delta^{18}O$), in agreement with earlier studies by Chiogna et al. (2014) and Cano-Paoli et al. (2019). For the GNIR data, we applied the error propagation analysis only to those datasets for which the uncertainty of the isotopic measurements was published (e.g., Halder et al., 2013; Rank et al., 2018). Analytical uncertainties and references for the GNIR data are reported in Table S2.

The Matlab scripts (MathWorks, Massachusetts, USA) used to compute the parameters and their uncertainties for the three regression methods, to propagate the error considering only the error in

the dependent variable and both in the dependent and independent variable are provided in the supporting information.

2.5. Data analysis

In order to compare the results obtained through the OLS regression with those deriving from RMA and MA methods, we computed the difference in the slopes ($slope_{OLS} - slope_{RMA/MA}$) and the intercepts ($intercept_{OLS} - intercept_{RMA/MA}$), as well as the percentage increase (Eq. 8):

$$percentage\ increase = \left(100\ \frac{slope_{RMA/MA}}{slope_{OLS}}\right) - 100 \quad (8)$$

Similarly to Crawford et al. (2014) and Boschetti et al. (2019), we used the Student's t-test (or the Mann-Whitney rank sum test in case of non-normally distributed data) to determine whether the differences between the slopes were statistically significant ($p \leq 0.05$).

Then, we investigated the relationships between regression parameters and differences in slopes and intercepts with statistical indices of the stream water datasets and catchment characteristics by Spearman rank correlation analysis. The statistical indices included sample size, δ^2H and $\delta^{18}O$ ranges, coefficients of variation of δ^2H and $\delta^{18}O$, and r computed between δ^2H and $\delta^{18}O$. The catchment characteristics included catchment area, mean annual precipitation, mean annual air temperature, elevation of the stream water sampling sites, latitude, and longitude of the stream water sampling sites (Table 1). Correlations with $p \leq 0.05$ were considered statistically significant. All data analyses were performed using Microsoft Office Excel (Microsoft Corporation, USA) and Matlab.

3. Results

3.1. Relationships between δ^2H and $\delta^{18}O$ of different water types in selected catchments in Italy

Most of the isotopic data from the selected catchments in north-eastern Italy plotted along the GMWL (Fig. 3). Rainfall samples from Posina, Rio Vauz, Noce Bianco, and Saldur had a large variability in δ^2H and $\delta^{18}O$ and plotted very close to the GMWL, with no outliers. Indeed, the four slopes and intercepts obtained with the OLS regression were very similar to the GMWL slope (8.0) and intercept (10.0) (Table 2). As expected, snow, ice, and melt waters were more depleted in heavy isotopes compared to summer rainfall from the same catchments, and some samples slightly deviated from the GMWL (Fig. 3b). The parameters $slope_{OLS}$ and $intercept_{OLS}$ of snow, ice, and melt waters differed from the same parameters determined for summer rain water, and while recent snow in Noce Bianco had a larger slope and intercept compared to GMWL, the melt water in the same catchment had a smaller slope and a negative intercept (Table 2). Sampled stream waters had smaller variability than rainfall (Posina, Rio Vauz, Noce Bianco, and Saldur) and snow, ice, and melt waters (Rio Vauz, Noce Bianco and Saldur). The parameters $slope_{OLS}$ and $intercept_{OLS}$ varied considerably, with a minimum slope of 3.9 (Po at Pontelagoscuro) and a maximum of 9.3 (one sampling site in Vermigliana) (Fig. 3 and Table 2). Most of the stream water from Posina, Rio Vauz, Noce Bianco, and Saldur plotted along the GMWL (only for the small Ressi catchment some of the samples plotted above the GMWL). Conversely, stream water in the Vermigliana, Po, and Adige rivers displayed some scatter and some samples deviated from the GMWL. As expected, groundwater, spring water, and soil water generally exhibited an isotopic variability similar to stream water collected in the same catchment (i.e., Rio Vauz and Ressi), whereas $slope_{OLS}$ and $intercept_{OLS}$ varied considerably with some waters having slopes (e.g., two springs in Rio Vauz and one spring in Noce Bianco; Table 2) much smaller than the slope of GMWL.

The error propagation analysis applied to the OLS regression showed that the variability in the isotopic data cannot be explained only by the uncertainty in the measurements. Indeed, for 67.2% of the datasets from north-eastern Italy (n=61, Tables 1 and 2), the propagated error in slopes and intercepts was smaller than their standard deviations. Considering the measurement precision (i.e., the average standard deviation of repeated measurements) as analytical uncertainty, we found for

more than 80% of the datasets from north-eastern Italy, a propagated error in slopes and intercepts smaller than their standard deviations. For 55.2% of the GNIR datasets (n=29, Table S2), the propagated error in slopes and intercepts was smaller than their standard deviations.

3.2. Differences between the OLS, RMA and MA regressions

For all three regression methods, rainfall had similar slopes (ranges for slopes were 7.5-8.1, 7.7-8.3 and 7.9-8.4 for OLS, RMA and MA, respectively; n=4 sampling sites) and intercepts (ranges for intercepts were 7.9-14.8, 9.4-16.2 and 10.6-17.7 for OLS, RMA and MA, respectively; n=4) determined for the δ^2H-$\delta^{18}O$ relationship (Table 2 and Fig. 4). As expected, we observed that minimum and maximum slopes and intercepts were the smallest for the OLS regression and the largest for the MA regression. This increasing pattern in slopes and especially intercepts for the RMA and MA regressions compared to the classical OLS method was definitely more evident when considering the other water types (Fig. 4). Slopes and intercepts for the δ^2H-$\delta^{18}O$ relationship of snow, ice, and melt waters (n=5 sampling sites) obtained by the RMA and MA regression were larger than the ones computed by the OLS method, but this pattern was not very clear due to the small variability in the slopes and intercepts (Table 2). Conversely, large variations in slopes and intercepts determined by the three regression methods were found for stream ($slope_{OLS}$ from 2.5 up to 9.3, $slope_{RMA}$ from 4.3 up to 10.9, $slope_{MA}$ from 4.7 up to 31.8, n=54 sampling sites) and spring waters ($slope_{OLS}$ from 3.9 up to 7.9, $slope_{RMA}$ from 7.1 up to 10.5, $slope_{MA}$ from 7.7 up to 28.5, n=8). For instance, the largest variation was observed for a stream water sampling site in the Vermigliana with slope varying from 2.5±1.3 ($slope_{OLS}$±standard deviation), 9.0±14.3 ($slope_{RMA}$±standard deviation) and up to 31.8±28.5 ($slope_{MA}$±standard deviation), and a spring water sampling site in Noce Bianco with slope varying from 3.8±4.1 (OLS), to 10.5±6.4 (RMA) and 28.5±14.5 (MA). An increase in slopes and intercepts from the OLS to RMA and MA regression method was also found for the δ^2H-$\delta^{18}O$ relationship of shallow groundwater (n= 12 sampling sites) and soil water (n=12) (Fig. 4 and Table 2).

Relationships between $slope_{OLS}$ (or $intercept_{OLS}$) and slopes (or intercepts) determined by the RMA and MA methods confirmed that RMA- and MA-based parameters were much larger compared to the ones determined by OLS (Fig. 5). The overestimation was very large when comparing MA to OLS parameters, and the differences were particularly marked for the intercepts (Fig. 5d). For rainfall, the differences between the regression methods were limited, as also shown in Fig. 4, whereas for shallow groundwater and soil waters large differences were more common for extreme $slope_{OLS}$ values (i.e., greater than 9 or lower than 6). The differences between the OLS parameters with the slopes and the intercepts determined by the RMA and MA methods were very large for some streams and springs (Fig. 5). However, we did not observe specific (e.g., geographical or climatic) patterns in the scattered overestimation for the various water types.

For each sampling site and water type, we quantified the percentage of increase in the slopes (Fig. 6) and the intercepts for the comparison between the RMA and MA regressions with the OLS method. Percentage increases in the slopes were small and quite similar for rainfall (median: 1.6% and 3.1% computed between OLS and RMA, and OLS and MA, respectively) and snow, ice, and melt waters (median: 1.5% and 3.0% computed between OLS and RMA, and OLS and MA, respectively). Median percentage increases in the slopes were also alike for spring and soil waters (about 4.5% and 9.0%, computed between OLS and RMA, and OLS and MA, respectively). For shallow groundwater, median percentage increase in the slopes was 8.8% and 18.2% (computation considering OLS and RMA, and between OLS and MA, respectively), while for stream waters medians reached 10.2% (between OLS and RMA slopes) and 20.8% (between OLS and MA slopes). Furthermore, it should be noted that, for all the water types, median percentage increases computed between OLS and RMA slopes were about half of median percentage increases calculated considering OLS and MA slopes (Fig. 6).

The analysis of the uncertainty in the regression parameters for each dataset (n=95) allowed us to determine whether the differences in the slopes and intercepts were significant. We found that for rainfall (n=4), snow, ice and melt waters (n=5) datasets, all the differences in the slopes and

intercepts were non-significant and smaller that their standard deviations (Fig. 7). The greatest proportion of datasets for which the differences between slopes and intercepts were larger than their standard deviations was observed for stream water (up to 70.4%, n=54), followed by groundwater (up to 66.7%, n=12), springs (up to 37.5%, n=8), and soil water (up to 16.7%, n=12). For stream water, springs, and groundwater, there were significant ($p \leq 0.05$) differences in the slopes; conversely, a similar difference was not found for soil water (Fig. 7a). As expected, the proportion of the differences between OLS and RMA parameters greater than slope and intercept standard deviations were lower than the proportions obtained considering the differences between OLS and MA parameters. The proportions obtained considering the differences in the slopes greater than the standard deviations (Fig. 7a) were very similar to the proportions obtained considering the differences in the intercepts (Fig. 7b), except for small variations in the proportions observed for groundwater and soil water. However, these discrepancies between the proportions for slopes and intercepts occurred only for few groundwater and soil water sites, possibly stemming from the intrinsic relationship existing between the two regression parameters, as described in Eq. 5.

3.3. Relationships between the differences in the slopes and the intercepts with the characteristics of the datasets

We observed small *r* values for two springs and several stream sampling sites, which led to large and negative differences between $slope_{OLS}$ and $slope_{RMA}$ (or $slope_{MA}$) (Fig. 8a,b). However, the magnitude of *r* (and therefore the differences in the slopes) seemed independent from the water type; indeed, except for stream water, the other water types had *r* values greater than 0.9, and differences between $slope_{OLS}$ and $slope_{RMA}$ (or $slope_{MA}$) were very close to 0. The relationship between sample size and the differences between $slope_{OLS}$ and $slope_{RMA}$ (or $slope_{MA}$) showed that, for small number of samples (<100), the differences in the slopes could be either very small (e.g., for rainfall, snow, ice and melt water, and soil water) or very large (e.g., for some spring water, and stream waters), while for large sample sizes the differences were usually small and close to 0 (Fig.

8c,d). The relationship between $\delta^{18}O$ range and the differences in the slopes indicates that, for waters having a large (mainly temporal) variability (>6 ‰ in $\delta^{18}O$) in the isotopic composition (e.g., rainfall and snow, ice and melt waters), the differences in the slopes were very close to 0 (Fig. 8e,f). Conversely, for stream waters, springs, and groundwater sites with small $\delta^{18}O$ ranges (<4 ‰), the differences between $slope_{OLS}$ and $slope_{RMA}$ (or $slope_{MA}$) were either small or very large. The relationships depicted in Fig. 8 (differences in the slopes vs. *r*, sample size, and $\delta^{18}O$ range) were also reproduced for the differences in the intercepts (Fig. S1). As expected, we found that the resulted relationships and patterns in Fig. S1 were very similar to the ones observed in Fig. 8.

The Spearman correlation analysis performed between statistics of stream water data and the differences in the slopes and the intercepts (Table 3) confirms the strong relationships already seen in Fig. 8 and S1. We found positive and significant correlations ($p<0.001$) between sample size and the differences in the slopes and the intercepts (Table 3). The correlations determined for the differences between $slope_{OLS}$ and $slope_{RMA}$ (or $slope_{MA}$) and $\delta^{2}H$ and $\delta^{18}O$ ranges were also positive, although weak. Furthermore, the correlations were significant when we considered the differences in the slopes, but non-significant between the differences in the intercepts and $\delta^{2}H$ range (but $p<0.1$). No significant correlations were observed between the differences in the slopes and the intercepts with coefficients of variation of $\delta^{2}H$ and $\delta^{18}O$ (Table 3).

Compared to the dataset statistics, catchment characteristics did not noticeably affect the differences in the slopes and the intercepts (Table 3). Indeed, the correlations between the differences in the slopes and the intercepts with catchment area, elevation, and longitude of the stream and river water sampling sites were non-significant (ρ_s values were weak or very weak). However, we observed weak but significant correlations between the differences in the slopes and the intercepts with mean annual precipitation ($p<0.01$), and between mean annual air temperature and the differences in the intercepts ($p<0.05$). We found a positive and moderate correlation ($p<0.001$) between latitude and the differences in slopes and intercepts. An inspection of the relationship among these parameters

showed that the statistical significance was mainly driven by stream sampling sites in the Vermigliana, Presanella, Sava, Kokra, and Posina catchments.

4. Discussion

4.1. Comparison of OLS, RMA and MA regressions applied to the δ^2H-$\delta^{18}O$ relationship

As expected by the mathematical structure of the three regression methods (Helsel and Hirsch, 2002; Keles, 2018), the largest slopes and intercepts were obtained by the MA regression, followed by slopes computed by the RMA method, and finally by the OLS regression (Fig. 4 and 5). Indeed, percentage increases in the slopes were all positive, and greater when considering OLS and MA (Fig. 6b) than OLS and RMA (Fig. 6a). We found for rainfall, snow, ice and melt waters data that the differences between the slopes and the intercepts determined by the three methods were very small (differences in the slopes varied between -0.40 and -0.04 ($slope_{OLS}$ and $slope_{RMA}$), and between -0.81 and -0.08 ($slope_{OLS}$ and $slope_{MA}$), Fig. 8) and similar to values found by Crawford et al. (2014) for precipitation data collected in central Europe. Conversely, for other water types (particularly for some stream and spring datasets), we observed that the differences in the regression parameters were even greater than those reported by Crawford et al. (2014), and sometimes greater than the standard deviations of slopes and intercepts (Fig. 7).

Furthermore, based on previous findings for precipitation data from coastal sites which are likely affected by kinetic fractionation (Crawford et al., 2014), we expected to find marked differences in the slopes and intercepts computed by the three methods for soil water isotopic data, which are usually more prone to evaporation processes. Indeed, some soil water samples had a clear evaporative signature (negative deuterium excess, Dansgaard (1964)), while others plotted close to the LMWL and GMWL (Fig. 3), likely reflecting the seasonality in evaporation as well as in the isotopic composition of local precipitation (Benettin et al., 2018). Despite this variability in the isotopic composition of soil water, we found that differences in slopes and the intercepts determined by the OLS, RMA, and MA regressions were usually small, non-significant and lower than their

standard deviations (Fig. 7). Therefore, based on our selected soil water datasets collected in continental study areas, we tend to exclude an influence of kinetic fractionation on the differences in the slopes and intercepts obtained by the three regression methods.

4.2. Factors influencing the differences in the slopes and the intercepts

Compared to previous studies (e.g., Hughes and Crawford, 2012; Crawford et al., 2014; Boschetti et al., 2019), our results indicate that the magnitude of the differences in the slopes and intercepts obtained by the three methods is primarily due to the correlation coefficient, *r*, computed between δ^2H and $\delta^{18}O$, regardless of the water type (Fig. 8a,b and S1a,b, Table 3). Therefore, the larger the correlation between δ^2H and $\delta^{18}O$ data, the smaller the differences among the parameters determined by the three regression methods.

Our results also show that for large sample sizes and $\delta^{18}O$ ranges, the differences in OLS, RMA, and MA fittings were usually small, regardless of the water type (Fig. 8 and S1). Conversely, for datasets with a small sample size and a small variability (expressed by $\delta^{18}O$ ranges) in the isotopic composition, the differences in the slopes and intercepts were more erratic, probably due to a large influence of measurement errors and/or high-leverage data (i.e., data points with extreme $\delta^{18}O$ values; Crawford et al., 2014). Because spring and stream waters are supposed to be more influenced by mixing processes rather than evaporation, and not all the datasets showed large differences in the regression parameters computed by the three methods, we argue that a dampened variability in the isotopic signature of a specific water source, combined with the measurement errors in δ^2H and $\delta^{18}O$, could lead to different results in the regression based on the applied method. For instance, a dampened variability in the isotopic composition was observed for samples collected from stream waters in the Posina and the Vermigliana, and from a spring in the Noce Bianco (Fig. 3), but the (small) isotopic variability was still larger than the propagated errors. Furthermore, we exclude that evaporation processes affected the sampled waters of Posina and Noce Bianco because deuterium excess was rarely below 8.0 (data not reported). However, we also note that the dampened isotopic

variability could be biased by the small sample size and the sampling design which could not capture the true range in the isotopic composition of surface waters. In addition, the correlation analysis showed that the isotopic ranges (which consider the difference between the largest and smallest values in the dataset) had a more significant correlation with differences in the slopes and the intercepts than the coefficients of variation had (Table 3), probably because the latter describe just about the dispersion around the mean isotopic composition.

The correlation analysis performed for stream water datasets also showed moderate and significant correlations between the differences in the slopes and the intercepts with the latitude of the sampling sites and mean annual precipitation of the catchments (Table 3). The inspection of the relationship between latitude of the sampling sites and differences in the slopes and the intercepts showed that the correlation was mainly driven by few sampling sites (i.e., Vermigliana, Presanella, Sava, Kokra and Posina), apparently with different catchment characteristics, but with *r* values smaller than 0.8. Due to the different characteristics of the catchments in terms of area, climate, and elevation of the sampling sites, we are not able to formulate plausible explanations (except for the poor relationships between δ^2H and $\delta^{18}O$) for the large differences among the parameters obtained by the OLS, RMA and MA methods.

Overall, the correlation analysis (Table 3) revealed that the differences in the slopes and the intercepts of stream waters were mainly affected by the statistical characteristics of the isotopic datasets rather than by the physical and climatic features of the catchments. However, this analysis was performed only for stream waters in continental sites in Europe and, therefore, our findings should be validated in other study areas in arid climates (as done for precipitation by Hughes and Crawford, 2012) or at the global scale (Crawford et al., 2014; Nan et al., 2019).

4.3. Recommendations for the application of the different regression methods in isotope hydrology

A literature review on the application of the OLS, RMA, and MA regression methods provides a multitude of studies in various disciplines, spanning from biology to astronomy. Many of these studies (e.g., Isobe et al., 1990; Smith, 2009; Kilmer and Rodriguez, 2017) tried to define some guidelines for the use of these regression methods depending on the investigated variables. However, previous research did not converge towards a unique set of guidelines because, before any application of the linear regression, a researcher should thoroughly examine the nature of the relationship between the two variables (i.e., cause vs. effect and asymmetric vs. symmetric partitioning of the variation) and quantify the measurement errors.

In general, the RMA and MA methods should be adopted in the presence of measurement errors for both the *x* and *y* variables. However, many studies recommended caution in the use of the RMA and MA regressions. For instance, Smith (2009) suggested to use the OLS method if the variation can be partitioned asymmetrically into the *x* and *y* variables, and the RMA if the variation should be treated symmetrically. Kilmer and Rodriguez (2017) specifically analysed the problem of the measurement error in allometry, and they concluded that it is preferable to use the OLS regression compared to the RMA, even when there are large measurement errors because a correction for slope attenuation usually can be adopted. Conversely, Isobe et al. (1990) and Boschetti et al. (2019) indicated the EIV regression models as preferable over OLS, RMA, and MA in case the nature of the variability is mainly due to measurement errors. In addition, in the RMA regression, the slope does not depend on *r* but on its sign, and therefore the former cannot help to explain the underlying relationship between the two variables (Isobe et al., 1990).

The MA regression is rarely applied (compared to OLS and the RMA methods) because the uncertainty in the MA slopes is generally greater than the uncertainties simulated with other methods (Isobe et al., 1990). The MA parameters sometimes are very large (in some cases, e.g., in Tables 2 and S1, they are almost unrealistic), and more sensitive to outliers and data points with high leverage compared to the OLS and RMA regressions (Crawford et al., 2014).

Based on our findings and on available isotope hydrology studies, before the application of the regression to the δ^2H-$\delta^{18}O$ relationship for both precipitation and other water types, we recommend to analyse the correlation between the two isotopes and the presence of outliers (and investigate their origin) and properly consider the measurement errors (e.g., by the analysis of the propagated errors). Then, we suggest to compute the regression lines based on the OLS, the RMA, and MA methods, and examine whether the isotopic variability is greater than the propagated errors. Finally, the resulting slopes should be compared considering the uncertainty in the estimates.

In case of small measurement errors and no significant differences between the slopes, we suggest the application of the widely used OLS regression. Conversely, if the computed slopes are significantly different, we recommend to investigate the possible reason (e.g., large measurement errors, dampened isotopic variability or presence of outliers), and then choose the RMA over the MA regression, especially as the latter is very sensitive to the presence of outliers or data with high leverage (Crawford et al., 2014). In case of very large measurement errors, an EIV approach should also be considered (Boschetti et al., 2019).

5. Conclusions

Recent studies compared the slopes and intercepts obtained for isotope precipitation data using the OLS regression with the parameters determined by the application of the RMA and the MA methods. Despite this recent research in isotope hydrology, no previous studies investigated the differences among the OLS, RMA, and MA regressions for water types prone to evaporation, mixing, and redistribution processes. Therefore, in this work, we quantified the differences in the slopes and intercepts computed by the OLS, RMA, and MA methods for various water types, and investigated whether the magnitude of the differences was affected by water type, dataset statistics, and/or by geographical/climatic characteristics of the selected datasets.

As expected by the mathematical structure of the three regression methods, we found that for all water types the MA regression always produced the largest slopes and intercepts whereas the OLS

method determined the smallest ones. The largest differences in the slopes and the intercepts were found for the isotopic data of some springs and streams. Conversely, for rainfall, snow, ice and melt water datasets, all the differences in the slopes and intercepts were smaller than their standard deviations. The largest proportion of datasets for which the differences between slopes and intercepts were greater than their standard deviations was observed for stream water, followed by groundwater, springs, and soil water. Our results show that the correlation between δ^2H and $\delta^{18}O$ is the main driver of the differences in the slopes and intercepts determined by the three regression methods, regardless of the water type; the stronger the correlation between δ^2H and $\delta^{18}O$ of the datasets, the smaller was the difference in the slopes (and the intercepts).

Based on our findings, in isotope hydrology applications we recommend to consider the measurement errors for both δ^2H and $\delta^{18}O$ and the presence of outliers, and to test whether the slopes computed by the OLS, RMA, and MA regressions are significantly different. In case of small measurement errors and no significant differences between the slopes, we suggest the application of the OLS regression. Conversely, if the computed slopes are significantly different, we recommend investigating the possible reasons for such discrepancies and preferring the RMA over the MA approach, as the latter tends to be more sensitive to data with high leverage.

Acknowledgements

CM and GZ acknowledges the financial support provided by Fondazione Cassa di Risparmio di Padova e Rovigo ("Ecohydrological Dynamics and Water Pathways in Forested Catchments", Bando Starting Grants 2015). Research in Rio Vauz and Posina was supported by the project "Giovani Studiosi – Ricerche di carattere innovative e di eccellenza proposte da giovani non strutturati, decreto rettorale n. 800-2011, 23/03/2011, University of Padova", the grant "Bando 2014 per il finanziamento di attrezzature scientifiche finalizzate alla ricerca" (University of Padova), the project "Ecohydrological Dynamics and Water Pathways in Forested Catchments" (Bando Starting Grants 2015, Fondazione Cassa di Risparmio di Padova e Rovigo), and the Italian

MIUR Project (PRIN 2017) “WATer mixing in the critical ZONe: observations and predictions under environmental changes - WATZON” (national coordinator: Marco Borga). GC, FC, ME and DP thank the BayIntAn program of the Bavarian Research Alliance (“Messung und Modellierung hydrologischer und geomorphologischer Prozesse in hochalpinen Einzugsgebieten”).

Authors contributions

DP conceived the original idea of testing alternative regression methods on water isotopic data different from precipitation. GZ, CM, and DP designed the research. CM prepared the datasets; GZ, CM, and GC conducted the data analysis. GZ and CM prepared the manuscript draft. All the authors contributed to the manuscript editing. MB funded the research. CM and GZ have contributed equally to this work.

References

Argiriou A.A., Lykoudis S., 2006. Isotopic composition of precipitation in Greece. Journal of Hydrology, 327, 486-495. DOI: 10.1016/j.jhydrol.2005.11.053

Benettin P., Volkmann T.H.M., von Freyberg J., Frentress J., Penna D., Dawson T.E., Kirchner J.W., 2018. Effects of climatic seasonality on the isotopic composition of evaporating soil waters. Hydrology and Earth System Sciences, 22(5), 2881–2890. DOI: 10.5194/hess-22-2881-2018

Boschetti T., Cifuentes J., Iacumin P., Selmo E., 2019. Local Meteoric Water Line of Northern Chile (18° S–30° S): An application of error-in-variables regression to the oxygen and hydrogen stable isotope ratio of precipitation. Water, 11, 791. DOI: 10.3390/w11040791

Cano-Paoli K., Chiogna G., Bellin A., 2019. Convenient use of electrical conductivity measurements to investigate hydrological processes in Alpine headwaters. Science of the Total Environment, 685, 37-49. DOI: 10.1016/j.scitotenv.2019.05.166

Cantrell, C.A. 2008. Technical Note: Review of methods for linear least-squares fitting of data and application to atmospheric chemistry problems. Atmospheric Chemistry and Physics, 8, 5477–5487.

Carr J.R., 2012. Orthogonal regression: a teaching perspective. International Journal of Mathematical Education in Science and Technology, 43:1, 134-143. DOI: 10.1080/0020739X.2011.573876

Carturan L., Zuecco G., Seppi R., Zanoner T., Borga M., Carton A., Dalla Fontana G., 2016. Catchment-scale permafrost mapping using spring water characteristics. Permafrost and Periglacial Processes, 27, 253-270. DOI: 10.1002/ppp.1875

Chiogna G., Santoni E., Camin F., Tonon A., Majone B., Trenti A., Bellin A., 2014. Stable isotope characterization of the Vermigliana catchment. Journal of Hydrology, 509, 295–305. DOI: 10.1016/j.jhydrol.2013.11.052

Chiogna G., Skrobanek P., Narany T.S., Ludwig R., Stumpp C., 2018. Effects of the 2017 drought on isotopic and geochemical gradients in the Adige catchment, Italy. Science of the Total Environment, 645, 924–936. DOI: 10.1016/j.scitotenv.2018.07.176

Craig H., 1961. Isotopic variations in meteoric waters. Science, 133, 1702-1703. DOI: 10.1126/science.133.3465.1702

Crawford J., Hollins S.E., Meredith K.T., Hughes C.E., 2017. Precipitation stable isotope variability and subcloud evaporation processes in a semi-arid region. Hydrological Processes, 31, 20-34. DOI: 10.1002/hyp.10885

Crawford J., Hughes C.E., Lykoudis S., 2014. Alternative least squares methods for determining the meteoric water line, demonstrated using GNIP data. Journal of Hydrology, 519, 2331-2340. DOI: 10.1016/j.jhydrol.2014.10.033

Dansgaard W., 1964. Stable isotopes in precipitation. Tellus, 16, 436–468. DOI: 10.1111/j.2153-3490.1964.tb00181

Engel M., Penna D., Bertoldi G., Dell'Agnese A., Soulsby C., Comiti F., 2016. Identifying run-off contributions during melt-induced run-off events in a glacierized alpine catchment. Hydrological Processes, 30, 343-364. DOI: 10.1002/hyp.10577

Evaristo J., Jasechko S., McDonnell J.J., 2015. Global separation of plant transpiration from groundwater and streamflow. Nature, 525, 91–94. DOI: 10.1038/nature14983

Feigelson E.D., Babu G.J., 1992. Linear regression in astronomy II. The Astrophysical Journal, 397, 55-67.

Florea L., Bird B., Lau J.K., Wang L., Lei Y., Yao T., Thompson L.G., 2017. Stable isotopes of river water and groundwater along altitudinal gradients in the High Himalayas and the Eastern Nyainqentanghla Mountains. Journal of Hydrology: Regional Studies, 14, 37–48. DOI: 10.1016/j.ejrh.2017.10.003

Fornasini P., 2008. The uncertainty in physical measurements: An introduction to data analysis in the physics laboratory. Springer-Verlag New York, 289 pp. DOI: 10.1007/978-0-387-78650-6

González-Trinidad J., Pacheco-Guerrero A., Júnez-Ferreira H., Bautista-Capetillo C., Hernández-Antonio A., 2017. Identifying groundwater recharge sites through environmental stable isotopes in an alluvial aquifer. Water, 9, 569. DOI: 10.3390/w9080569

Guastini E., Zuecco G., Errico A., Castelli G., Bresci E., Preti F., Penna D., 2019. How does streamflow response vary with spatial scale? Analysis of controls in three nested Alpine catchments. Journal of Hydrology, 570, 705-718. DOI: 10.1016/j.jhydrol.2019.01.022

Halder J., Decrouy L., Vennemann T.W., 2013. Mixing of Rhône River water in Lake Geneva (Switzerland–France) inferred from stable hydrogen and oxygen isotope profiles. Journal of Hydrology, 477, 152–164. DOI: 10.1016/j.jhydrol.2012.11.026

Halder J., Terzer S., Wassenaar L.I., Araguás-Araguás L.J., Aggarwal P.K., 2015. The Global Network of Isotopes in Rivers (GNIR): integration of water isotopes in watershed observation and riverine research. Hydrology and Earth System Sciences, 19, 3419–3431. DOI: 10.5194/hess-19-3419-2015

Harper W.V., 2014. Reduced major axis regression: Teaching alternatives to least squares. In K. Makar, B. de Sousa, & R. Gould (Eds.), Sustainability in statistics education. Proceedings of the Ninth International Conference on Teaching Statistics (ICOTS9, July, 2014), Flagstaff, Arizona, USA. Voorburg, The Netherlands: International Statistical Institute.

Helsel D.R., Hirsch R.M., 2002. Statistical methods in water resources. In: Techniques of Water-Resources Investigations of the United States Geological Survey, Book 4, Hydrologic Analysis and Interpretation, 510 pp.

Hervé-Fernández P., Oyarzún C., Brumbt C., Huygens, D., Bodé S., Verhoest N.E.C., Boeckx, P., 2016. Assessing the 'two water worlds' hypothesis and water sources for native and exotic evergreen species in south-central Chile. Hydrological Processes, 30, 4227-4241. DOI: 10.1002/hyp.10984

Hollins S.E., Hughes C.E., Crawford J., Cendón D.I., Meredith K.T., 2018. Rainfall isotope variations over the Australian continent – Implications for hydrology and isoscape applications. Science of The Total Environment, 645, 630–645. DOI: 10.1016/j.scitotenv.2018.07.082

Hughes C.E., Crawford J., 2012. A new precipitation weighted method for determining the meteoric water line for hydrological applications demonstrated using Australian and global GNIP data. Journal of Hydrology, 464–465, 344–351. DOI: 10.1016/j.jhydrol.2012.07.029

International Atomic Energy Agency (IAEA), 1992. Statistical treatment of data on environmental isotopes in precipitation. Technical Reports Series No. 331, IAEA, Vienna.

Isobe T., Feigelson E.D., Akritas M.G., Babu G.J., 1990. Linear regression in astronomy I. The Astrophysical Journal, 364, 104-113.

Javaux M., Rothfuss Y., Vanderborght J., Vereecken H., Brüggemann N., 2016. Isotopic composition of plant water sources. Nature, 536. DOI: 10.1038/nature18946

Kaseke K.F., Wang L., Wanke H., Turewicz V., Koeniger P., 2016. An analysis of precipitation isotope distributions across Namibia using historical data. Plos One, 11(5), e0154598. DOI: 10.1371/journal.pone.0154598

Keleş T., 2018. Comparison of classical least squares and orthogonal regression in measurement error models. International Online Journal of Educational Sciences, 10(3), 204-219. DOI: 10.15345/iojes.2018.03.013

Kilmer J.T. Rodríguez R.L., 2017. Ordinary least squares regression is indicated for studies of allometry. Journal of Evolutionary Biology, 30, 4–12. DOI: 10.1111/jeb.12986

Klaus J., McDonnell J.J., Jackson C.R., Du E., Griffiths N.A., 2015. Where does streamwater come from in low-relief forested watersheds? A dual-isotope approach. Hydrology and Earth System Sciences, 19, 125-135. DOI: 10.5194/hess-19-125-2015

Koeniger P., Marshall J.D., Link T., Mulch A., 2011. An inexpensive, fast, and reliable method for vacuum extraction of soil and plant water for stable isotope analyses by mass spectrometry. Rapid Communications in Mass Spectrometry, 25, 3041-3048. DOI: 10.1002/rcm.5198

Le Duy N., Heidbüchel I., Meyer H., Merz B., Apel H. 2018. What controls the stable isotope composition of precipitation in the Mekong Delta? A model-based statistical approach. Hydrology and Earth System Sciences, 22, 1239–1262. DOI: 10.5194/hess-22-1239-2018

Marchina C., Bianchini G., Natali C., Pennisi M., Colombani N., Tassinari R., Knöller K., 2015. The Po river water from the Alps to the Adriatic Sea (Italy): new insights from geochemical and isotopic ($\delta^{18}O$-δD) data. Environmental Sciences and Pollution Research, 22, 5184–5203. DOI:

10.1007/s11356-014-3750-6

Marchina C., Bianchini G., Knöller K., Natali C., Pennisi M., Colombani N., 2016. Natural and anthropogenic variations in the Po river waters (northern Italy): insights from a multi-isotope approach. Isotope in Environmental and Health Studies, 52, 649–672. DOI: 10.1080/10256016.2016.1152965

Marchina C., Natali C., Fazzini M., Fusetti M., Tassinari R., Bianchini G., 2017. Extremely dry and warm conditions in northern Italy during the year 2015: effects on the Po river water. Rendiconti Lincei, 28(2), 281–290. DOI: 10.1007/s12210-017-0596-0

Marchina C., Natali C., Bianchini G., 2019. The Po river water isotopes during the drought condition of the year 2017. Water, 11, 150. DOI: 10.3390/w11010150

Miljević N., Golobočanin D., Ogrinc N., Bondžić A., 2008. Distribution of stable isotopes in surface water along the Danube River in Serbia. Isotopes in Environmental and Health Studies, 44, 137-148. DOI: 10.1080/10256010802066141

Nan Y., Tian F., Hu H., Wang L., Zhao S., 2019. Stable isotope composition of river waters across the world. Water, 11, 1760. DOI: 10.3390/w11091760

Natali C., Bianchini G., Marchina C., Knöller K., 2016. Geochemistry of the Adige River water from the Eastern Alps to the Adriatic Sea (Italy): evidences for distinct hydrological components and water-rock interactions. Environmental Sciences and Pollution Research, 23(12), 11677-11694. DOI: 10.1007/s11356-016-6356-3

Oiro S., Comte J.-C., Soulsby C., Walraevens K., 2018. Using stable water isotopes to identify spatio-temporal controls on groundwater recharge in two contrasting East African aquifer systems. Hydrological Sciences Journal, 63, 862–877. DOI: 10.1080/02626667.2018.1459625

Pawellek F., Frauenstein F., Veizer J., 2002. Hydrochemistry and isotope geochemistry of the upper Danube River. Geochimica et Cosmochimica Acta, 66(21), 3839–3854. DOI: 10.1016/S0016-7037(01)00880-8

Peng T., Chen K., Zhan W., Lu W., Tong L.J., 2015. Use of stable water isotopes to identify hydrological processes of meteoric water in montane catchments. Hydrological Processes, 29, 4957-4967. DOI: 10.1002/hyp.10557

Penna D., Engel M., Bertoldi G., Comiti F., 2017a. Towards a tracer-based conceptualization of meltwater dynamics and streamflow response in a glacierized catchment. Hydrology and Earth System Sciences, 21, 23-41. DOI: 10.5194/hess-21-23-2017

Penna D., Engel M., Mao L., Dell'Agnese A., Bertoldi G., Comiti F., 2014. Tracer-based analysis of spatial and temporal variations of water sources in a glacierized catchment. Hydrology and Earth System Sciences, 18, 5271-5288. DOI: 10.5194/hess-18-5271-2014

Penna D., Oliviero O., Assendelft R., Zuecco G., van Meerveld I., Anfodillo T., Carraro V., Borga M., Dalla Fontana G., 2013. Tracing the water sources of trees and streams: isotopic analysis in a small pre-alpine catchment. Procedia Environmental Sciences, 19, 106-112. DOI: 10.1016/j.proenv.2013.06.012

Penna D., Stenni B., Šanda M., Wrede S., Bogaard T.A., Gobbi A., Borga M., Fischer B.M.C.,

Bonazza M., Chárová Z., 2010. On the reproducibility and repeatability of laser absorption spectroscopy measurements for δ^2H and $\delta^{18}O$ isotopic analysis. Hydrology and Earth System Sciences, 14, 1551–1566. DOI: 10.5194/hess-14-1551-2010

Penna D., Stenni B., Šanda M., Wrede S., Bogaard T.A., Michelini M., Fischer B.M.C., Gobbi A., Mantese N., Zuecco G., Borga M., Bonazza M., Sobotková M., Čejková B., Wassenaar L.I., 2012. Technical Note: Evaluation of between-sample memory effects in the analysis of δ^2H and $\delta^{18}O$ water samples measured by laser spectroscopes. Hydrology and Earth System Sciences, 16, 3925-3933. DOI: 10.5194/hess-16-3925-2012

Penna D., van Meerveld H.J., Oliviero O., Zuecco G., Assendelft R.S., Dalla Fontana G., Borga M., 2015. Seasonal changes in runoff generation in a small forested mountain catchment. Hydrological Processes, 29, 2027-2042. DOI: 10.1002/hyp.10347

Penna D., van Meerveld H.J., Zuecco G., Dalla Fontana G., Borga M., 2016. Hydrological response of an Alpine catchment to rainfall and snowmelt events. Journal of Hydrology, 537, 382-397. DOI: 10.1016/j.jhydrol.2016.03.040

Penna D., Zuecco G., Crema S., Trevisani S., Cavalli M., Pianezzola L., Marchi L., Borga M., 2017b. Response time and water origin in a steep nested catchment in the Italian Dolomites. Hydrological Processes, 31, 768-782. DOI: 10.1002/hyp.11050

Putman A.L., Fiorella R.P., Bowen G.J., Cai Z., 2019. A global perspective on local meteoric water lines: Meta-analytic insight into fundamental controls and practical constraints. Water Resources Research, 55, 6896–6910. DOI: 10.1029/2019WR025181

Qu S., Chen X., Wang Y., Shi P., Shan S., Gou J., Jiang P., 2018. Isotopic characteristics of precipitation and origin of moisture sources in Hemuqiao catchment, a small watershed in the lower reach of Yangtze River. Water, 10, 1170. DOI: 10.3390/w10091170

Rank D., Papesh W., Tesh R., 2006. Isotope tracing of hydrological processes in large river basins: Danube study. In: Interfacing the Past and the Future of Ecology and Water Management in a Large European River, 36th International Conference: Danube. River. Life, Proceedings, 388-393.

Rank D., Wyhlidal S., Schott K., Weigand S., Oblin A., 2018. Temporal and spatial distribution of isotopes in river water in Central Europe: 50 years experience with the Austrian network of isotopes in rivers. Isotopes in Environmental and Health Studies, 54, 115-136. DOI: 10.1080/10256016.2017.1383906

Rollinson H.R., 1993. Using geochemical data: evaluation, presentation, interpretation. Routledge: Longman Geochemistry Series, 384 pp.

Rozanski K., Araguás-Araguás L., Gonfiantini R., 1993. Isotopic patterns in modern global precipitation. Climate change in continental isotopic records (P.K. Swart, K.L. Lohmann, J. McKenzie, S. Savin, Eds). Geophysical Monograph 78, American Geophysical Union, Washington, DC, 1-37.

Sánchez-Murillo R., Aguirre-Dueñas E., Gallardo-Amestica M., Moya-Vega P., Birkel C., Esquivel-Hernández G., Boll J., 2015. Isotopic characterization of waters across Chile. In Andean hydrology, Rivera, D.A., Godoy-Faundez, A., Lillo-Saavedra, M., Eds.; CRC Press: New York, NY, USA, 2018; (9) 205–230.

Sharma A., Kumar K., Singh A. K., Metha P., 2017. Oxygen, deuterium, and strontium isotope characteristics of the Indus River water system. Geomorphology, 284, 5-16. DOI: 10.1016/j.geomorph.2016.12.014

Shi M., Wang S., Argiriou A.A., Zhang M., Guo R., Jiao, R., Kong J., Zhang Y., Qiu X., Zhou S., 2019. Stable isotope composition in surface water in the upper Yellow River in Northwest China. Water, 11, 967. DOI: 10.3390/w11050967

Smith R.J., 2009. Use and misuse of the reduced major axis for line-fitting. American Journal of Physical Anthropology, 140, 476–486. DOI: 10.1002/ajpa.21090

Tan H., Wen X., Rao W., Bradd J., Huang J., 2016. Temporal variation of stable isotopes in a precipitation–groundwater system: implications for determining the mechanism of groundwater recharge in high mountain–hills of the Loess Plateau, China. Hydrological Processes, 30, 1491-1505. DOI: 10.1002/hyp.10729

Volk W., 1958. Applied Statistics for Engineers. McGraw-Hill Book Company Inc., New York.

Vreča P., Malenšek N., 2016. Slovenian Network of Isotopes in Precipitation (SLONIP) – a review of activities in the period 1981–2015. Geologija, 59, 67-84. DOI: 10.5474/geologija.2016.004

Wang B., Zhang H., Liang X., Li X., Wang F., 2019. Cumulative effects of cascade dams on river water cycle: Evidence from hydrogen and oxygen isotopes. Journal of Hydrology, 568, 604-610. DOI: 10.1016/j.jhydrol.2018.11.016

Wassenaar L.I, Athanasopoulos P., Hendry M.J., 2011. Isotope hydrology of precipitation, surface and ground waters in the Okanagan Valley, British Columbia, Canada. Journal of Hydrology, 411, 37-48. DOI: 10.1016/j.jhydrol.2011.09.032

Xu T., Sun X., Hong H., Wang X., Cui M., Lei G., Gao L., Liu J., Lone M.A., Jiang X., 2019. Stable isotope ratios of typhoon rains in Fuzhou, Southeast China, during 2013–2017. Journal of Hydrology, 570, 445-453. DOI: 10.1016/j.jhydrol.2019.01.017

Zannoni D., Steen-Larsen H.C., Rampazzo G., Dreossi G., Stenni B., Bergamasco A., 2019. The atmospheric water cycle of a coastal lagoon: An isotope study of the interactions between water vapor, precipitation and surface waters. Journal of Hydrology, 572, 630-644. DOI: 10.1016/j.jhydrol.2019.03.033

Zuecco G., Carturan L., De Blasi F., Seppi R., Zanoner T., Penna D., Borga M., Carton A., Dalla Fontana G., 2019a. Understanding hydrological processes in glacierized catchments: Evidence and implications of highly variable isotopic and electrical conductivity data. Hydrological Processes, 33, 816-832. DOI: 10.1002/hyp.13366

Zuecco G., Penna D., Borga M., 2018. Runoff generation in mountain catchments: long-term hydrological monitoring in the Rio Vauz Catchment, Italy. Cuadernos de Investigación Geográfica, 44(2), 397-428. DOI: 10.18172/cig.3327

Zuecco G., Penna D., Borga M., van Meerveld H.J., 2016. A versatile index to characterize hysteresis between hydrological variables at the runoff event timescale. Hydrological Processes, 30, 1449-1466. DOI: 10.1002/hyp.10681

Zuecco G., Penna D., van Meerveld H.J., Hopp L., Dalla Fontana G., Borga M., 2014. Comparison of two different types of throughfall collectors. Die Bodenkultur, 65 (3-4), 51-56.

Zuecco G., Rinderer M., Penna D., Borga M., van Meerveld H.J., 2019b. Quantification of subsurface hydrologic connectivity in four headwater catchments using graph theory. Science of the Total Environment, 646, 1265-1280. DOI: 10.1016/j.scitotenv.2018.07.26

Tables

Catchment	Area (km^2)	Mean annual precipitation (mm)	Mean annual temperature (°C)	Sampling elevation for stream/river waters (m a.s.l.)	Data availability	Type of data (number of samples)	References for catchments and datasets
Rio Vauz Subcatchment: BCC	1.9	1220	4.1	1910, 1932	2010-2017	P (34), SIM (107), SW (477), SP (356), GW (157), SOW (22)	Penna et al. (2016), Penna et al. (2017b), Zuecco et al. (2018), Guastini et al. (2019)
Posina (at Stancari) Subcatchments: Posina at Bazzoni, Ressi	116	1708	10.3	387, 453, 598	2012-2018	P (55), SW (1387), GW (643), SOW (297)	Penna et al. (2013), Zuecco et al. (2014), Penna et al. (2015), Zuecco et al. (2016)
Noce Bianco	8.4	1233	-0.5	2298	2012-2016	P (40), SIM (130), SW (487), SP (52)	Carturan et al. (2016), Zuecco et al. (2019a)
Saldur	35.0	526	6.6	2150, 2333	2011-2013	P (46), SW (117), SP (72)	Penna et al. (2014), Engel et al. (2016), Penna et al. (2017a)
Vermigliana	104	1440	2.9	974, 1176, 1220, 1226, 1342, 1436, 1546, 1793	2011-2012	SW (201), GW (17)	Chiogna et al. (2014), Cano-Paoli et al. (2019)
Adige (Andriano)	2642	718	7.7	242	2015-2017	SW (9)	Natali et al. (2016), Chiogna et al. (2018)
Adige (Verona)	10900	837	14	67	2015-2017	SW (9)	Natali et al. (2016), Chiogna et al. (2018)
Adige (Boara Pisani)	11954	718	13.3	5	2015-2017	SW (9)	Natali et al. (2016), Chiogna et al. (2018)
Po (Pontelagoscuro)	70000	666	13.6	0	2012-2017	SW (27)	Marchina et al. (2015), Marchina et al. (2016), Marchina et al. (2019)

Table 1. Main characteristics of the selected catchments in northern-eastern Italy and brief description of the available data. Water types are abbreviated as in: P - rainfall; SIM - snow, ice and melt water; SW - surface water (streams and rivers); SP - spring water; GW - groundwater; SOW - soil water.

Catchment	Water type	OLS		RMA		MA	
		slope (SE)	intercept (SE)	slope (SE)	intercept (SE)	slope (SE)	intercept (SE)
Rio Vauz Subcatchment: BCC	P	7.93 (0.20)	11.44 (2.03)	8.01 (0.20)	12.25 (2.04)	8.09 (0.21)	13.04 (2.05)
	SIM	8.21 (0.14)	11.44 (1.94)	8.33 (0.14)	13.10 (1.95)	8.45 (0.14)	14.74 (1.97)
	SW	6.79 (0.38), 6.93 (0.18)	-4.24 (4.81), -2.94 (2.33)	7.70 (0.39), 7.80 (0.19)	7.39 (4.96), 8.09 (2.40)	8.70 (0.43), 8.75 (0.21)	20.16 (5.43), 20.12 (2.62)
	SP	5.80 (0.26), 4.55 (0.56)	-17.66 (3.30), -32.76 (7.06)	7.14 (0.27), 7.15 (0.62)	-0.82 (3.46), 0.22 (7.81)	8.72 (0.32), 11.12 (0.87)	19.16 (4.03), 50.45 (10.98)
	GW	6.76 – 9.06 (0.24 – 0.70)	-5.36 – 21.52 (2.95 – 9.88)	7.47 – 9.21 (0.24 – 0.72)	3.27 – 23.32 (2.95 – 10.08)	7.62 – 9.97 (0.25 – 0.76)	5.78 – 31.51 (2.98 – 10.70)
	SOW	8.34 (0.40), 4.64 (0.60)	16.58 (4.56), -24.35 (5.74)	8.38 (0.40), 5.16 (0.62)	17.02 (4.56), -19.56 (5.88)	8.42 (0.41), 5.69 (0.66)	17.44 (4.58), -14.60 (6.33)
Posina (at Stancari) Subcatchments: Posina at Bazzoni, Ressi	P	8.12 (0.23)	14.75 (2.09)	8.29 (0.23)	16.24 (2.10)	8.45 (0.23)	17.70 (2.13)
	SW	5.61 – 7.75 (0.07 – 0.64)	-6.06 – 12.79 (0.62 – 5.71)	8.01 – 8.16 (0.07 – 0.70)	15.26 – 16.19 (0.62 – 6.19)	8.57 – 11.41 (0.08 – 0.91)	19.66 – 45.43 (0.65 – 8.11)
	GW	6.09 – 7.74 (0.25 – 0.62)	-2.92 – 12.43 (2.21 – 5.12)	7.81 – 8.17 (0.26 – 0.64)	11.31 – 16.00 (2.25 – 5.24)	8.19 – 9.95 (0.28 – 0.68)	14.38 – 31.32 (2.37 – 5.60)
	SOW	6.56 – 10.40 (0.18 – 1.14)	-4.59 – 29.51 (1.03 – 8.95)	6.88 – 11.06 (0.18 – 1.16)	-3.31 – 34.68 (1.03 – 9.09)	7.20 – 11.76 (0.18 – 1.21)	-2.02 – 40.09 (1.03 – 9.51)
Noce Bianco	P	7.53 (0.27)	7.86 (2.49)	7.70 (0.27)	9.44 (2.51)	7.88 (0.27)	11.01 (2.55)
	SIM	6.17 – 9.08 (0.18 – 0.52)	-12.07 – 28.49 (2.60 – 7.14)	6.57 – 9.43 (0.18 – 0.53)	-6.56 – 32.89 (2.61 – 7.26)	6.98 – 9.79 (0.18 – 0.55)	-0.96 – 37.36 (2.64 – 7.59)
	SW	7.68 (0.08)	7.51 (1.17)	7.90 (0.08)	10.58 (1.18)	8.12 (0.09)	13.64 (1.20)
	SP	3.85 (4.89), 7.82 (0.24)	-42.89 (65.50), 7.63 (2.96)	10.52 (5.92), 7.98 (0.24)	46.38 (79.27), 9.63 (2.97)	28.53 (13.28), 8.15 (0.25)	287.48 (177.72), 11.61 (3.02)
Saldur	P	8.03 (0.13)	9.67 (1.37)	8.07 (0.13)	10.13 (1.38)	8.11 (0.13)	10.58 (1.38)
	SW	7.90 (0.40),	9.47	8.16 (0.41),	13.18 (5.96),	8.41 (0.42),	16.89 (6.09),

		8.13 (0.21)	(5.91), 12.87 (3.10)	8.37 (0.21)	16.34 (3.12)	8.60 (0.22)	19.81 (3.19)
	SP	6.99 – 7.89 (0.35 – 0.59)	-4.30 – 8.92 (4.80 – 8.83)	7.34 – 8.07 (0.35 – 0.60)	0.83 – 11.98 (4.83 – 8.94)	7.69 – 8.25 (0.36 – 0.62)	6.02 – 15.04 (4.91 – 9.25)
Vermigliana	SW	2.51 – 9.26 (0.87 – 1.84)	-62.63 – 25.61 (10.89 – 23.31)	7.60 – 10.34 (0.91 – 2.30)	3.04 – 38.04 (11.35 – 29.14)	9.15 – 31.76 (1.03 – 6.50)	23.30 – 307.59 (12.85 – 82.35)
	GW	5.04 (1.31)	-28.00 (16.30)	7.15 (1.42)	-1.75 (17.66)	10.04 (1.84)	34.25 (22.91)
Adige (at Andriano)	SW	7.23 (0.85)	1.20 (10.73)	7.57 (0.86)	5.51 (10.86)	7.92 (0.89)	9.88 (11.22)
Adige (at Verona)	SW	7.80 (0.76)	8.39 (8.85)	8.05 (0.76)	11.35 (8.92)	8.30 (0.78)	14.31 (9.13)
Adige (at Boara Pisani)	SW	8.92 (1.91)	21.01 (21.84)	10.25 (1.97)	36.19 (22.58)	11.75 (2.18)	53.33 (25.03)
Po (at Pontelagoscuro)	SW	3.93 (0.77)	-26.98 (6.82)	5.50 (0.83)	-13.13 (7.37)	7.57 (1.06)	5.16 (9.39)

Table 2. Slopes, intercepts and their respective standard errors (SE) obtained by the application of the OLS, RMA and MA methods to the δ^2H-$\delta^{18}O$ relationship for different water types in the selected catchments in northern Italy. When there were more than two sampling sites for water type, we reported ranges in the slopes, intercepts and SE. Water types are abbreviated as in: P - rainfall; SIM - snow, ice and melt water; SW - surface water (streams and rivers); SP - spring water; GW - groundwater; SOW - soil water.

	Spearman rank correlation coefficients (ρ_s) for the relationships between differences in the slopes and the intercepts with statistical indices of the datasets and catchment characteristics				
Statistical indices:	**$slope_{OLS}$ - $slope_{RMA}$**	**$intercept_{OLS}$ - $intercept_{RMA}$**	**$slope_{OLS}$ - $slope_{MA}$**	**$intercept_{OLS}$ - $intercept_{MA}$**	**Number of sampling sites**
Sample size (-)	0.50***	0.50***	0.50***	0.49***	54
δ^2H range (‰)	0.28*	0.23	0.28*	0.24	54
$\delta^{18}O$ range (‰)	0.38**	0.36**	0.38**	0.36**	54
Coefficient of variation of δ^2H (-)	0.18	0.17	0.18	0.17	54
Coefficient of variation of $\delta^{18}O$ (-)	-0.06	-0.08	-0.06	-0.08	54
***r* computed between δ^2H and $\delta^{18}O$ (-)**	0.99***	0.98***	0.99***	0.98***	54
Catchment characteristics:					
Latitude (°)	0.56***	0.57***	0.56***	0.57***	54
Longitude (°)	0.14	0.17	0.14	0.16	54
Area (km^2)	0.24	0.30	0.24	0.30	41
Mean annual precipitation (mm)	-0.38**	-0.42**	-0.38**	-0.42**	47
Mean annual temperature (°C)	0.28	0.34*	0.28	0.34*	46
Elevation of the sampling site (m)	-0.20	-0.27	-0.20	-0.27	51

Significance codes: ***= $p \leq 0.001$; **= $p \leq 0.01$; *= $p \leq 0.05$.

Table 3. Spearman rank correlation coefficients for the relationships between differences in the slopes and the intercepts (computed with the OLS, RMA and MA methods) with statistical indices of the stream and river water datasets and catchment characteristics. Number of sampling sites for which data were available is indicated in last column.

Figures

Figure 1. Graphical rapresentation (modified from Crawford et al., 2014) of the three regression methods considered in this study: the OLS (Ordinary Least Squares), the RMA (Reduced Major Axis), and the MA (Major Axis) methods.

Figure 2. Location of the selected catchments in northern Italy. Mountainous areas are indicated in grey.

Figure 3. Dual-isotope plots for the δ^2H-$\delta^{18}O$ relationship for various water types sampled in the selected Italian catchments: a) Posina (including Ressi); b) Rio Vauz (including BCC); c) Noce Bianco; d) Saldur; e) Vermigliana; f) Po and Adige. Characteristics of the selected catchments and the collected samples are reported in Table 1.

Figure 4. Data plots with a) the slopes and b) the intercepts calculated with the OLS, RMA and MA regressions for the different water types. The three different methods are represented with three different filling colours (OLS-white; RMA-grey; MA-black).

Figure 5. Scatter plots between a) $slope_{OLS}$ and $slope_{RMA}$; b) $intercept_{OLS}$ and $intercept_{RMA}$; c) $slope_{OLS}$ and $slope_{MA}$; d) $intercept_{OLS}$ and $intercept_{MA}$.

Figure 6. Percentage increases (reported in a logarithmic scale) in the slopes computed considering a) OLS and RMA, and b) OLS and MA for the various water types. Bars represent median percentage increases, while error bars indicate minimum and maximum percentage increases.

Figure 7. Proportion of datasets, grouped by water type, for which the differences between a) slopes and b) intercepts computed with the three regression methods (OLS-RMA and OLS-MA) were larger

than the standard deviations. In a), we indicated above each bar whether we found a significant difference between the slopes by the application of the Student's t-test or the Mann-Whitney rank sum test (significant codes: NS=p>0.05; *= p≤ 0.05; **= p≤ 0.01; ***= p≤ 0.001).

Figure 8. Scatter plots between a) Pearson correlation coefficient, *r*, computed between δ^2H and $\delta^{18}O$ and difference in the slopes (OLS-RMA); b) *r* computed between δ^2H and $\delta^{18}O$ and difference in the slopes (OLS-MA); c) sample size and difference in the slopes (OLS-RMA); d) sample size and difference in the slopes (OLS-MA); e) $\delta^{18}O$ range (difference between maximum and minimum) and difference in the slopes (OLS-RMA); f) $\delta^{18}O$ range and difference in the slopes (OLS-MA).

Declaration of interests

☒ The authors declare that they have no known competing financial interests or personal relationships that could have appeared to influence the work reported in this paper.

☐The authors declare the following financial interests/personal relationships which may be considered as potential competing interests:

Abstract

The Ordinary Least Squares (OLS) regression is the most common method for fitting the δ^2H-$\delta^{18}O$ relationship. Recently, various studies compared the OLS regression with the Reduced Major Axis (RMA) and Major Axis (MA) regression for precipitation data. However, no studies have investigated so far the differences among the OLS, RMA and MA regressions for water types prone to evaporation,

mixing, and redistribution processes. In this work, we quantified the differences in terms of slopes and intercepts computed by the OLS, RMA, and MA methods for rainfall, snow and ice, stream, spring, groundwater, and soil water, and investigated whether the magnitude of such differences is significant and dependent on the water type, the datasets statistics, geographical or climatic characteristics of the study catchments.

Our results show that the differences between the regression methods were largest for the isotopic data of some springs and some stream waters. Conversely, for rainfall, snow, ice, and melt waters datasets, all the differences were small and, particularly, smaller than their standard deviation. Slopes and intercepts computed using the different regression methods were statistically different for stream water (up to 70.4%, n=54), followed by groundwater, springs, and soil water. The results of this study indicate that a thorough analysis of the δ^2H-$\delta^{18}O$ relationship in isotope hydrology studies is recommended, as well as considering the measurement errors for both δ^2H and $\delta^{18}O$, and the presence of outliers. In case of small measurement errors and no significant differences between the slopes, we suggest the application of the widely used OLS regression. Conversely, if the computed slopes are significantly different, we recommend investigating the possible reasons for such discrepancies and prefer the RMA over the MA approach, as the latter tends to be more sensitive to data with high leverage (i.e., data points with extreme $\delta^{18}O$ values).

Keywords: stable water isotopes; Ordinary Least Squares regression; Major Axis regression; stream water; Global Meteoric Water Line; catchment.

Figures

Figure 1. Graphical rapresentation (modified from Crawford et al., 2014) of the three regression methods considered in this study: the OLS (Ordinary Least Squares), the RMA (Reduced Major Axis), and the MA (Major Axis) methods.

Figure 2. Location of the selected catchments in northern Italy. Mountainous areas are indicated in grey.

Figure 3. Dual-isotope plots for the δ^2H-$\delta^{18}O$ relationship for various water types sampled in the selected Italian catchments: a) Posina (including Ressi); b) Rio Vauz (including BCC); c) Noce Bianco; d) Saldur; e) Vermigliana; f) Po and Adige. Characteristics of the selected catchments and the collected samples are reported in Table 1.

Figure 4. Data plots with a) the slopes and b) the intercepts calculated with the OLS, RMA and MA regressions for the different water types. The three different methods are represented with three different filling colours (OLS-white; RMA-grey; MA-black).

Figure 5. Scatter plots between a) $slope_{OLS}$ and $slope_{RMA}$; b) $intercept_{OLS}$ and $intercept_{RMA}$; c) $slope_{OLS}$ and $slope_{MA}$; d) $intercept_{OLS}$ and $intercept_{MA}$.

Figure 6. Percentage increases (reported in a logarithmic scale) in the slopes computed considering a) OLS and RMA, and b) OLS and MA for the various water types. Bars represent median percentage increases, while error bars indicate minimum and maximum percentage increases.

Figure 7. Proportion of datasets, grouped by water type, for which the differences between a) slopes and b) intercepts computed with the three regression methods (OLS-RMA and OLS-MA) were larger than the standard deviations. In a), we indicated above each bar whether we found a significant difference between the slopes by the application of the Student's t-test or the Mann-Whitney rank sum test (significant codes: NS=$p>0.05$; *= $p\leq 0.05$; **= $p\leq 0.01$; ***= $p\leq 0.001$).

Figure 8. Scatter plots between a) Pearson correlation coefficient, *r*, computed between δ^2H and $\delta^{18}O$ and difference in the slopes (OLS-RMA); b) *r* computed between δ^2H and $\delta^{18}O$ and difference in the slopes (OLS-MA); c) sample size and difference in the slopes (OLS-RMA); d) sample size and difference in the slopes (OLS-MA); e) $\delta^{18}O$ range (difference between maximum and minimum) and difference in the slopes (OLS-RMA); f) $\delta^{18}O$ range and difference in the slopes (OLS-MA).

Highlights

- Uncertainty in slopes of mixed waters is not explained by the experimental error
- Stream and spring isotopic data have significant differences in the slopes
- Evaporated soil water does not significantly affect the δ^2H-$\delta^{18}O$ relationship

Credit author statement

DP conceived the original idea of testing alternative regression methods on water isotope data different from precipitation. GZ, CM, and DP designed the research. CM prepared the datasets; GZ, CM, and GC conducted the data analysis. GZ and CM prepared the manuscript draft. All the authors contributed to the manuscript editing. MB funded the research. CM and GZ have contributed equally to this work.

Supplementary material

Catchment	Sample size	OLS		*r*	RMA		MA	
		slope	intercept		slope	intercept	slope	intercept
DANUBE - Engelhartszell	112	7.38	2.58	0.98	7.50	3.90	7.61	5.20
DANUBE - Hainburg	412	7.37	2.42	0.98	7.54	4.31	7.70	6.17
DANUBE - Medvedovo	29	7.02	-1.90	0.94	7.44	2.65	7.87	7.32
DANUBE - Tulcea	78	5.41	-17.06	0.92	5.86	-12.54	6.33	-7.91
DANUBE - Vienna	321	7.54	4.62	0.98	7.71	6.48	7.88	8.33

DRAU - Neubruecke	109	7.57	6.33	0.99	7.66	7.42	7.76	8.50
ILL - Gisingen	237	7.75	7.59	0.98	7.91	9.51	8.05	11.40
INN - Kirchbichl	126	7.75	7.29	0.98	7.86	8.87	7.98	10.42
INN - S'Chanf	194	7.84	7.18	0.98	8.00	9.27	8.16	11.34
INN - Schaerding	214	7.73	6.78	0.99	7.81	7.73	7.88	8.66
JALOVECKY CREEK - Dolina	277	7.46	7.24	0.90	8.29	16.70	9.19	26.92
JALOVECKY CREEK - Ondrasova	109	7.09	2.02	0.92	7.73	9.17	8.40	16.72
KOKRA - Mouth	17	6.32	-2.97	0.62	10.24	34.31	16.48	93.74
LEITHA - Deutsch-Brodersdorf	112	7.50	5.06	0.96	7.77	7.93	8.05	10.81
MAAS - Eijsden	23	3.85	-20.81	0.90	4.27	-17.94	4.67	-15.08
MARCH - Angern	127	6.16	-9.79	0.98	6.29	-8.65	6.41	-7.54
MUR - Spielfeld	189	7.36	3.85	0.96	7.64	6.89	7.92	9.94
PRESANELLA - Trentino - P3	25	6.93	-2.88	0.64	10.88	46.17	16.98	122.06
PRESENA - Trentino - P11	8	8.23	12.75	0.95	8.66	18.19	9.10	23.78
PRESENA - Trentino - P9	24	5.66	-19.59	0.80	7.04	-2.37	8.71	18.30
RHINE - Diepoldsau	293	7.63	4.67	0.89	8.55	16.28	9.56	28.97
RHINE - Lobith	23	6.45	-7.26	0.73	8.79	14.75	11.92	44.11
RHINE - Lustenau	115	7.78	8.15	0.99	7.89	9.50	7.99	10.82
RHINE - Weil	129	7.39	1.64	0.91	8.12	9.49	8.89	17.86
RHONE - Chancy	78	8.14	9.39	0.82	9.93	30.36	12.07	55.46
RHONE - Porte du Scex	294	7.28	-0.79	0.90	8.09	10.54	8.97	22.77
SALZACH - Salzburg	257	7.51	4.82	0.98	7.67	6.78	7.83	8.72
SAVA - Jesenice na Dolenjskem	37	6.55	-0.53	0.72	9.09	22.64	12.53	54.10

SAVA - Mostec	17	4.70	-17.33	0.64	7.30	6.35	11.22	42.00
SAVA - Smlednik	16	6.14	-5.09	0.68	9.05	22.67	13.27	62.80
SAVA - Sobec	16	3.86	-29.04	0.48	8.03	12.52	16.52	97.05
SCHELDE - S.V.Ouden Doel	21	5.14	-10.11	0.98	5.25	-9.57	5.36	-9.05
UHLIRSKA - Porsche Profile	126	6.40	-3.48	0.92	6.98	2.35	7.60	8.48
VAH - Liptovsky Mikulas	48	6.70	-2.12	0.95	7.09	2.00	7.48	6.20

Table S1. Samples size, Pearson correlation coefficient (*r*), slopes and intercepts obtained by the application of the OLS, RMA and MA methods to the δ^2H-$\delta^{18}O$ relation for stream water data retrieved by the GNIR database.

Catchment	**Analytical uncertainty**		**References**
	δ^2H (‰)	**$\delta^{18}O$ (‰)**	
DANUBE - Engelhartszell	1.0	0.10	Rank D., Wyhlidal S., Schott K., Weigand S., Oblin A., 2018. Temporal and spatial distribution of isotopes in river water in Central Europe: 50 years experience with the Austrian network of isotopes in rivers. *Isotopes in Environmental and Health Studies, 54, 115-136.* DOI: 10.1080/10256016.2017.1383906
DANUBE - Hainburg			
DANUBE - Medvedovo			
DANUBE - Tulcea			
DANUBE - Vienna			
DRAU - Neubruecke			
ILL - Gisingen			
INN - Kirchbichl			
INN - S'Chanf			

INN - Schaerding			
LEITHA - Deutsch-Brodersdorf			
MARCH - Angern			
MUR - Spielfeld			
RHINE - Diepoldsau			
RHINE - Lobith			
RHINE - Lustenau			
RHINE - Weil			
SALZACH - Salzburg			
KOKRA - Mouth	1.0	0.10	Ogrinc N., Kanduč T., Stichler W., Vreča P., 2008. Spatial and seasonal variations in $\delta^{18}O$ and δD values in the River Sava in Slovenia. *Journal of Hydrology, 359, 303-312.* DOI: 10.1016/j.jhydrol.2008.07.010
SAVA - Jesenice na Dolenjskem			
SAVA - Mostec			
SAVA - Smlednik			
SAVA - Sobec			
PRESANELLA - Trentino - P3	2.0	0.20	Chiogna G., Santoni E., Camin F., Tonon A., Majone B., Trenti A., Bellin A., 2014. Stable isotope characterization of the Vermigliana catchment. *Journal of Hydrology, 509, 295-305.* DOI: 10.1016/j.jhydrol.2013.11.052
PRESENA - Trentino - P11			
PRESENA - Trentino - P9			
RHONE - Chancy	0.4	0.07	Halder J., Decrouy L., Vennemann T.W., 2013. Mixing of Rhône River water in Lake Geneva (Switzerland-France) inferred from stable hydrogen and oxygen isotope profiles. *Journal of Hydrology, 477, 152–164.* DOI: 10.1016/j.jhydrol.2012.11.026
RHONE - Porte du Scex			
VAH - Liptovsky Mikulas	1.0	0.20	Povinec P.P., Zéenišová Z., Šivo S., Ogrinc N., Richtáriková M., Breier R., 2013. Radiocarbon and stable isotopes as groundwater tracers in the Danube river basin of SW Slovakia. *Proceedings of the 21st International Radiocarbon Conference. Radiocarbon, 55, 1017-1028.* DOI: 10.1017/S003382220005815X

Table S2. Analytical uncertainty considered in the error propagation analysis for stream water data retrieved by the GNIR database.

Fig. S1. Scatter plots between a) Pearson correlation coefficient, *r*, computed between δ^2H and $\delta^{18}O$ and difference in the intercepts (OLS-RMA); b) *r* computed between δ^2H and $\delta^{18}O$ and difference in the intercepts (OLS-MA); c) sample size and difference in the intercepts (OLS-RMA); d) sample size and difference in the intercepts (OLS-MA); e) $\delta^{18}O$ range (difference between maximum and

minimum) and difference in the intercepts (OLS-RMA); f) $\delta^{18}O$ range and difference in the intercepts (OLS-MA).